Signal Quality Classification of Impedance Plethysmogram and Ballistocardiogram for Pulse Transit Time Measurement

SHING-HONG LIU[1], TAI-SHEN HUANG[2,*], XIN ZHU[3], TAN-HSU TAN[4], JIA-JUNG WANG[5]
[1]Department of Computer Science and Information Engineering, Chaoyang University of Technology, Taichung City 41349,
TAIWAN

[2]Department of Industrial Design, Chaoyang University of Technology, Taichung City 41349,
TAIWAN

[3]Division of Information Systems, School of Computer Science and Engineering, University of Aizu, Aizu-Wakamatsu 965-8580,
JAPAN

[4]Department of Electrical Engineering, National Taipei University of Technology, Taipei 10608,
TAIWAN

[5]Department of Biomedical Engineering, I-Shou University, Kaohsiung 84001,
TAIWAN

**Corresponding Author*

Abstract: - Mobile health (mHealth) was developed ten years ago, which used wireless wearable devices to collect the many physiological messages in daily life, regardless of time and place, for some health services including monitoring chronic diseases and reducing the cost of empowering patients and families for handling their daily healthcare. However, the challenge for these measurements is the lower signal quality because users would measure their conditions not on a resting status. Now, the pulse transit time (PTT) is highly related to blood pressure has been proposed, which is acquired from the impedance plethysmography (IPG) and ballistocardiogram (BCG) measured by the weight-fat scale. However, the lower signal quality of IPG and BCG, lowers the accuracy of blood pressure. This study aims to use deep learning techniques to classify the signal quality of BCG and IPG signals. The reference PTTs were measured by the electrocardiogram (ECG) and photoplethysmogram (PPG). The signal quality of each segment was labeled with the error between proposed and reference PTTs. We used three signals, BCG, IPG, and differential IPG, as the input. The proposed one-dimensional stacking convolutional neural network and gait recursive unit (1-D CNN+GRU) model to approach the classification. The good performances achieved high accuracy (98.85%), recall (99.4%), precision (94.29%), and F1-score (96.78%). These results show the potential benefit of the signal quality classification for the PTT measurement.

Key-Words: - mHealth, signal quality, ballistocardiogram, impedance plethysmogram, pulse transit time, convolutional neural network.

Received: Septermber 13, 2023. Revised: July 11, 2024. Accepted: August 12, 2024. Published: September 11, 2024.

1 Introduction

Wireless and wearable devices are the major issue in mobile health (mHealth) because devices deal with some health services, including monitoring the conditions of chronic diseases, and reducing the cost of users for handling their daily healthcare without the limitations of time and place, [1]. Thus, many studies have developed innovative wearable devices in the past 10 years for taking care of patients, or health management of users. For example, the Apple watch has the functions of detecting the

arrhythmia by the electrocardiogram, and monitoring the blood oxygen saturation, [2]. The electrocardiography (ECG) patch, [3] and electromyography (EMG) patch, [4] have been proposed to monitor the condition of the heart and muscle in real-time. However, innovative mobile devices for different health care are very important research.

Blood pressure (BP) is the most important physiological parameter for healthcare in the home because it has direct and indirect relations with many chronic diseases, like hypertension, hyperlipidemia, heart failure, stroke, and kidney disease, etc. [5]. According to the World Health Organization's report, people must measure their BP daily and keep their systolic BP lower than 130 mmHg, [6]. The commercial and automatic sphygmomanometer uses either auscultatory or oscillometric methods, [7]. These methods all use an occlusive cuff wrapping around a user's upper arm to measure the BP. The disadvantage of these methods is uncomforting when the BP is measured. In the recent years, the cuffless BP measurements have been widely studied, [8]. According to the Moens-Korteweg equation, the pulse transit time (PTT) has a high relation with BP, [9]. Reference [10], showed the PTT by the ECG and photoplethysmogram (PPG). They found the relation between the PTT and BP change to be larger than 0.8. Reference, [11] used phonocardiography replacing the ECG, and PPG to measure the PTT and estimate the BP. Reference [12], used the tonometer measured at the wrist which was replaced with the PPG, and ECG to evaluate the blood pressure. Reference [13], used an impedance plethysmogram (IPG) measured at the forearm which replaced the PPG, and ECG to measure the PTT and estimate the BP. Reference [14], proposed innovative cuffless BP measuring methods with the ballistocardiogram (BCG) and IPG. The BCG and IPG signals can be measured from a commercial weight-fat scale. However, in these studies, we found a basic problem. The lower the quality of the signal, the lower the accuracy of blood pressure.

The quality of physiological signals generally is labeled by the manual marks of experts, [15]. However, the signal quality would depend on the experiences of experts. The rule-based method is to find some waveform characteristics and classify whether they fit the normal ranges or not, [16]. The disadvantage is how to define the accurate ranges which would be affected by the number of samples. Reference [17], transferred the pulses of PPG and differential PPG (DPPG) to an image and used a convolutional neural network (CNN) for the classification of signal quality. Its advantage was to transfer a one-dimension signal to a two-dimension image. Reference [18] showed some methods for signal quality classifications of ECG. We found that the deep learning methods classified the signal quality, which input would be a two-dimensional image. Thus, the complexity of bringing to practice will arise.

This study aims to propose a deep learning model for signal quality classification which uses the raw BCG and IPG signals as the input. The signal quality was labeled-labeled by the error of PTT measured from BCG and IPG. The PTT measured by the ECG and PPG was the reference. The BCG and IPG were measured by the self-made circuits when users were standing on the commercial weight-fat scale. The deep learning model was a stacking CNN plus a gate recursive unit (GRU). The output was one node, one representing good quality, and zero representing poor quality.

2 Methods

2.1 Experiment Protocol

This study employed 11 males and 6 females who were young and healthy subjects. Their ages were from 22 to 19 years (mean ± standard deviation, 20.2 ± 1.1 years), heights were from 186 to 152 cm (mean ± standard deviation, 166.1 ± 8.0 cm), and weights were from 115 to 43 kg (mean ± standard deviation, 62.8 ± 16.1 kg). The digital sphygmomanometer (HM-7320, Omron, Osaka, Japan) was used to measure the BPs as the reference. The self-made circuit was used to measure Lead I ECG and finger PPG of the left hand. $PTT_{ECG\text{-}PPG}$ was measured from the ECG and PPG which would be the standard PTT. The self-made circuits were used to measure the BCG and IPG signals, and which sensors were at a commercial body weight-fat scale (HBF-371, Omron, Osaka, Japan), [18]. The experiment procedure is mentioned below.

I. ECG, PPG, IPG, and BCG signals were measured for five minutes, and BP was measured once when subjects were standing on the weight-fat scale.
II. Subjects were running on a treadmill to raise the BP until the systolic BP was higher than the 20 mmHg of resting BP.
III. Subjects were standing on the weight-fat scale again, and ECG, PPG, IPG, and BCG signals were

measured for six minutes. Their BPs were measured once a minute.

IV. Subjects were measured four times. Each experiment would have a rest for at least a week.

2.2 Signal Processing and Segment

The sampling rate was 500 Hz. The 4th-order Butterworth bandpass filter with 0.5 Hz to 10 Hz bandwidth was used to remove the wandering baseline and high-frequency noise. The group delays of all signal groups were reduced by an 8th-order all-pass filter. Figure 1 shows these signals, ECG (blue), PPG (red), DPPG (pink), BCG (black), IPG (green), and differential IPG (DIPG, purple). The $PTT1_{BCG\text{-}IPG}$ is the interval between the J wave of BCG and the foot point of IPG, and the $PTT2_{BCG\text{-}IPG}$ is the interval between the J wave of BCG and the peak point of DIPG. The $PTT1_{ECG\text{-}PPG}$ is the interval between the R wave of ECG and the foot point of PPG, and the $PTT2_{ECG\text{-}PPG}$ is the interval between the R wave of ECG and the peak point of DPPG.

We used the error ratio (E) between $PTT2_{ECG\text{-}PPG}$ and $PTT2_{BCG\text{-}IPG}$ of each beat to define the signal quality.

$$E = \frac{PTT2_{ECG-PPG} - PTT2_{BCG-IPG} - Bias}{PTT2_{ECG-PPG}} \times 100\%, \quad (1)$$

where *Bias* is the time delay between ECG and BCG, [14]. By the trial and error method, we defined 30% of E as the threshold. When E is below the threshold, the pulse belongs to good quality, this cycle labeling as 1. Otherwise, the cycle is labeled as 0. Figure 2 shows the labels of pulses with the red line. We find that the second pulse belongs to poor quality because the foot of its IPG is at the wrong place. Because the PTT1 and PTT2 were extracted from the BCG, IPG, and DIPG, we used the three signals directly to classify the signal quality.

In the data segment, the window was 1024 points, the overlap was 512 points. In order to reduce the personal affection for the classification of signal quality, the BCG (blue), IPG (red), and DIPG (orange), were normalized, as shown in Figure 3. Because one segment has at least two PTTs, the segment was labeled as good or poor quality depending on all pulses in it belonging to all good or poor. The segment would be deleted when the pulses in it had different qualities. The numbers of good and poor samples were 3938 and 18682, a total of 22,620 samples.

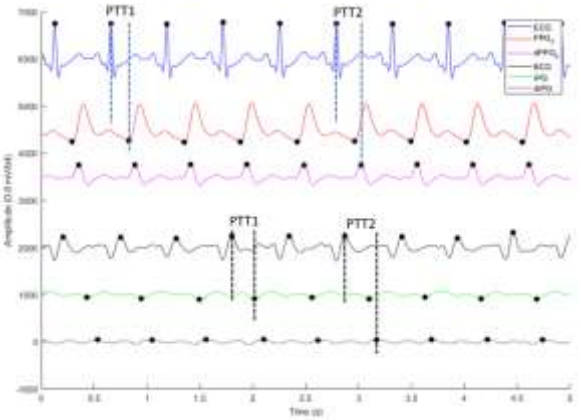

Fig. 1: PTT1 and PTT2 are defined by ECG (blue), PPG (red), DPPG (pink), BCG (black), IPG (green), and differential IPG (DIPG, purple)

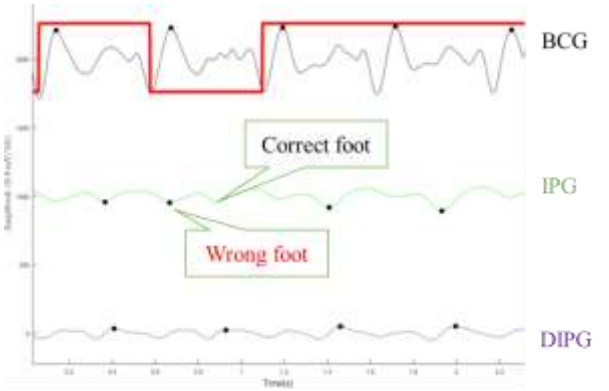

Fig. 2: The label of signal quality is the red line, When the pulse belongs to the good quality, its cycle is labeled as 1 (higher horizontal line). Otherwise, the label is 0 (lower horizontal line)

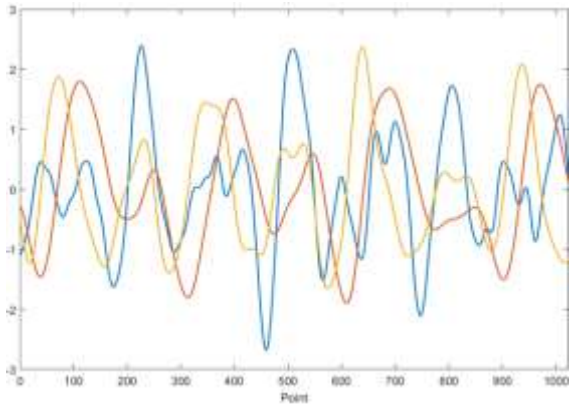

Fig. 3: The normalized BCG (blue), IPG (red), and DIPG (orange)

2.3 Signal Quality Classifier

A stacking CNN+GRU model was proposed to classify the signal quality as shown in Figure 4. The three channels, BCG, IPG, and DIPG signals, are the input. A time-distributed layer is separated into two parts that connect to two one-dimensional CNNs. The CNN has three layers, a maximal pool

layer, and a flattened layer. Then, a GRU is connected after the flattening layer. A full connection layer connects with the output layer of the GRU. In CNN layers, the number of filters is 32, the kernel sizes are 3, 5, and 13, respectively, and the stride is 2. In the maximal pooling layer, the kernel size is 2, and the stride is 2. The activation function is ReLU. The unit number of GRU is set to 1024. The batch size is set to 512, with the control reset gate and update gate using a sigmoid function and the hidden state using a tanh function. One node is in the output layer, and which activation function is the sigmoid function. One represents the good quality, and zero represents the poor quality. The threshold of output is 0.5. The dropout in the hidden layer is 0.5. The loss function is the binary Cross-Entropy function, and the Adam optimizer is used, with a learning rate of 0.0001.

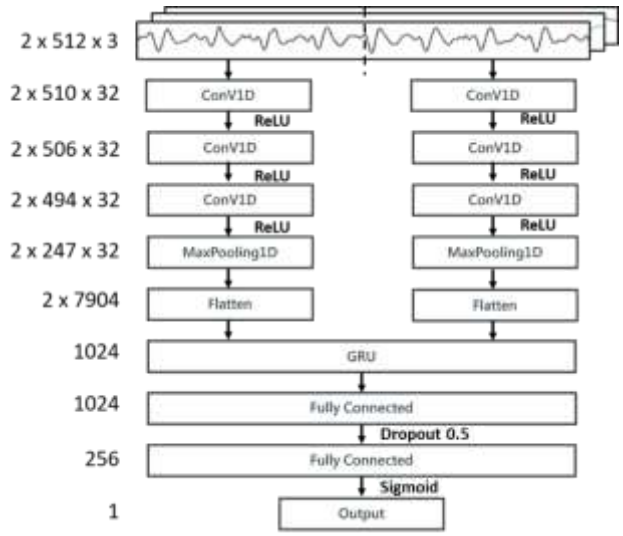

Fig. 4: The structure of the proposed stacking CNN+GRU model for the signal quality classification.

3 Results

An Intel Core i7-8700 CPU and a 186 GeForce GTX3070 GPU were used to evaluate the performance of the proposed method. The number of total samples was 22,620, and the numbers of training and testing samples were 15,834 and 6,786, respectively. The training samples were separated as the training and validation samples with 8 to 2.

The statistic of data is expressed as the mean ± standard deviation. The sensitivity, specificity, and accuracy are used to evaluate the performance of the model. In the fusion matrix, TP is true positive, FN is false negative, FP is false positive, and TN is true negative.

$$Sensitivity(\%) = \frac{TP}{(TP+FN)} \times 100\%, \quad (2)$$

$$Specificity(\%) = \frac{FP}{(FP+TN)} \times 100\% \quad (3)$$

$$Accuracy(\%) = \frac{TP+TN}{(TP+TN+FP+FN)} \times 100\%. \quad (4)$$

The accuracy curves of the stacking CNN+GRU model in the training (blue line) and validation (orange line) phases are shown in Figure 5(a). The loss curves are shown in Figure 5(b). We find that the accuracy approaches 0.97, and the loss value approaches 0.12 when the epoch is 14. The fusion matrix in the testing phase is shown in Figure 6, the numbers of TP, TN, FN, and FP are 1174, 5534, 7, and 71. The results of accuracy, sensitivity, and specificity are 98.9%, 99.4%, and 98.7%, respectively.

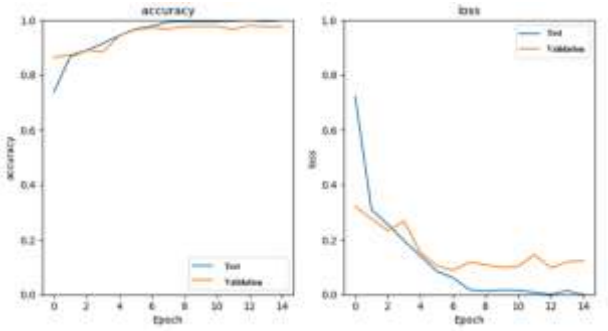

(a) (b)

Fig. 5: The results of the stacking CNN+GRU model in the training (blue) and validation (orange) phases, (a) the accuracy curves, (b) the loss curves

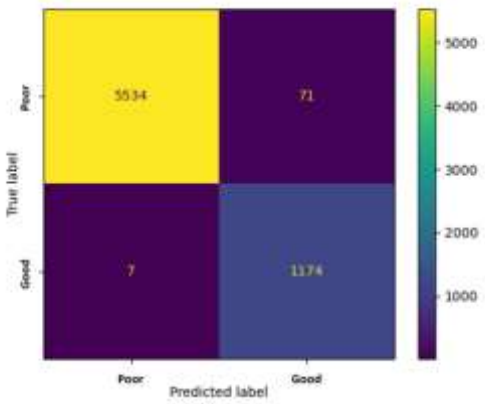

Fig. 6: The fusion matrix in the testing phase. The numbers of TP, TN, FN, and FP are 1174, 5534, 7, and 71

4 Discussions

The size of the segment would be an explored issue in this study. Because the sampling rate was 500 Hz, the minimum size of the segment was 512 points. Figure 7(a) shows the accuracy curves in the training (blue line) and validation (orange line) phases when the size of the segment is 512, and Figure 7(b) shows the loss curves. The accuracy approaches 0.92, and the loss value approaches 0.18 when the epoch is 4. Its performance is lower than the 1024 points of segment size. The reason would be that the rate of non-complete cycle is close to the full cycle. Although the signal quality within the non-complete cycle is poor, and the signal quality within the full cycle is good, this segment is also labeled as good quality. Thus, the model would recognize the signals with the poor quality as the good quality.

Figure 8(a) shows the accuracy curves in the training (blue line) and validation (orange line) phases when the size of the segment is 2048, and Figure 8(b) shows the loss curves. The accuracy approaches 0.98, and the loss value approaches 0.16 when the epoch is 14. This performance is very close to the 1024 points of segment size. But, the disadvantage was that the number of samples would decrease a lot. Because when the segment size is 2048 points, the number of full cycles would be 5 at least. According to the labeling rules, the rate of failed segments would increase. Therefore, we chose the 1024 points of segment size as the sample.

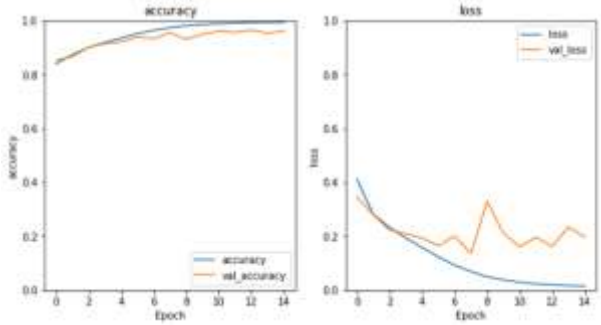

Fig. 7: The results of the stacking CNN+GRU model in the training (blue) and validation (orange) phases with a segment size of 512 points, (a) the accuracy curves, (b) the loss curves

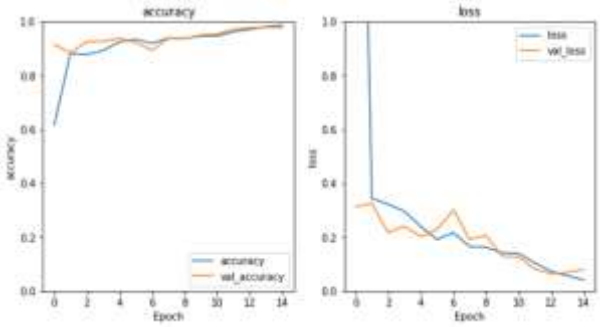

Fig. 8: The results of the stacking CNN+GRU model in the training (blue) and validation (orange) phases with a segment size of 2048 points, (a) the accuracy curves, (b) the loss curves

5 Conclusion

In the development of mHealth, wireless and wearable devices for monitoring physiological conditions every day have gotten attention. Now, PTT can be used to estimate the BP, which usually is measured by the ECG and PPG signals when subjects sitting on a chair or lying on the bed. When users are standing on the weight-fat scale to measure the PTT, the signals must have larger artificial motions. In this study, we proposed the stacking CNN+GRU model to classify the signal quality of BCG and IPG signals with the one-dimensional data. The accuracy approached to 98.9%. Thus, it has the potential benefit for BP measurement with the weight-fat scale when users standing on it. Therefore, this method could be applied in the mHealth in the future.

However, the major limitation of this study is that the subjects all were young and healthy people. They stood on the weight-fat scale more stable than the elderly. When users have Parkinson's disease or use assistive devices for standing, they cannot suit this method.

Acknowledgement:
This research was supported by the National Science and Technology Council, Taiwan, and JST Japan Collaborative Research Program, Grant Number: NSTC 113-2923-E-324 -001 -MY3, Grant Number JPMJKB2311, Japan.

References:

[1] B.M. Silva, J.J. Rodrigues, de la Torre Díez I, M. López-Coronado, K. Saleem, "Mobile-health: A review of current state in 2015," *J. Biomed. Inform.*, vol.56, pp. 265-72, 2015,https://doi.org/10.1016/j.jbi.2015.06.003

[2] How to use the Blood Oxygen app on Apple Watch, [Online]. https://support.apple.com/en-us/HT211027 (Accessed Date: December 2, 2012).

[3] S. S. Lobodzinski, "ECG patch monitors for assessment of cardiac rhythm abnormalities, " *Progress in Cardiovascular Diseases*, vol. 56, pp 224–229, 2013, https://doi.org/10.1016/j.pcad.2013.08.006.

[4] C. Kantarcigil, M. K. Kim, T. Chang, B. A. Craig, A. Smith, C. H. Lee, G. A. Malandraki, "Validation of a novel wearable electromyography patch for monitoring submental muscle activity during swallowing: a randomized crossover trial," *Journal of Speech, Language, and Hearing Research*, vol.63, pp 3293–3310, 2020, https://doi.org/10.1044/2020_JSLHR-20-00171.

[5] M.V. Williams, D.W. Baker, R.M. Parker, J. R. Nurss, "Relationship of functional health literacy to patients' knowledge of their chronic disease: a study of patients with hypertension and diabetes," *Arch. Intern. Med.*, vol.158, pp.166-172, 1998, https://doi.org/10.1001/archinte.158.2.166.

[6] A. M. Master, L.I. Dublin, H.H. Marks. "The normal blood pressure range and its clinical implications," *JAMA*. vol.143, pp.1464-1470, 1950, https://doi:10.1001/jama.1950.02910520006004.

[7] J.J. Carr, J.M. Brown, Introduction to Biomedical Equipment Technology, 4th ed.; Prentice Hall: City, Country, 2001; ISBN:0-13-010492-2.

[8] C. Ahlstrom, A. Johansson, F. Uhlin, T. Länne, P. Ask, "Noninvasive investigation of blood pressure changes using the pulse wave transit time: a novel approach in the monitoring of hemodialysis patients," *J. Artif. Organs*, vol.8, pp.192–197, 2015, https://doi.org/10.1007/s10047-005-0301-4.

[9] D.L. Newman, S.E. Greenwald, "Validity of the Moens-Korteweg equation," *The Arterial System*, pp. 109–115, 1978.

[10] G. Sharwood-Smith, J. Bruce, G. Drummond, "Assessment of pulse transit time to indicate cardiovascular changes during obstetric spinal anesthesia," *Br. J. Anaesth.*, vol. 96, pp.100–105, 2006, https://doi.org/10.1093/bja/aei266.

[11] J.Y.A. Foo, C.S. Lim, P. Wang, "Evaluation of blood pressure changes using vascular transit time," *Physiol. Meas.*, vol.27, pp.685–694, 2006, https://doi.org/10.1088/0967-3334/27/8/003.

[12] M. Park, H. Kang, Y. Huh, K.C. Kim, "Cuffless and noninvasive measurement of systolic blood pressure, diastolic blood pressure, mean arterial pressure and pulse pressure using radial artery tonometry pressure sensor with concept of Korean traditional medicine," *Proceedings of the 29th Annual International Conference of the IEEE Engineering in Medicine and Biology Society, Lyon*, France, 22–26 August 2007, pp. 3597–3600, 2007, https://doi.org/10.1109/IEMBS.2007.4353109.

[13] T. H. Huynh, R. Jafari, W.-Y. Chung, "Noninvasive cuffless blood pressure estimation using pulse transit time and impedance plethysmography," *IEEE Transactions on Biomedical Engineering*, vol. 66, pp 967–976, 2018.

[14] S.-H. Liu, Y.-R. Wu, W. Chen, C.-H. Su, C.-L. Chin, "Using ballistocardiogram and impedance plethysmogram for minimal contact measurement of blood pressure based on a body weight-fat scale," *Sensors*, vol.23, 2318, 2023, https://doi.org/10.3390/s23042318.

[15] C. Fischer, B. Domer, T. Wibmer, T. Penzel, "An algorithm for real-time pulse waveform segmentation and artifact detection in photoplethysmograms," *IEEE J. Biomed. Health Inform.*, vol.21, pp. 372–381, 2017. https://doi.org/10.1109/JBHI.2016.2518202.

[16] W. Karlen, K. Kobayashi, J.M. Ansermino, G.A. Dumont, "Photoplethysmogram signal quality estimation using repeated Gaussian filters and cross-correlation," *Physiol. Meas.*, vol. 33, pp.1617-1629, 2012, https://doi.org/10.1088/0967-3334/33/10/1617.

[17] H. Shin, "Deep convolutional neural network-based signal quality assessment for photoplethysmogram," *Computers in Biology and Medicine*, vol. 145, 105430, 2022, https://doi.org/10.1016/j.compbiomed.2022.105430.

[18] U. Satija, B. Ramkumar, M.S. Manikandan, "A review of signal processing techniques for electrocardiogram signal quality assessment," *IEEE Reviews in Biomedical Engineering*, vol.11, pp.36-52, 2018, https://doi.org/10.1109/RBME.2018.2810957.

Contribution of Individual Authors to the Creation of a Scientific Article (Ghostwriting Policy)

- Sing-Hong Liu carried out the concept and method.
- Tai-Shen Huang supported the subjects and prototype.
- Xin Zhu revised the English.
- Tan-Hsu Tan implemented the Algorithm of deep learning model.
- Jia-Jung Wang write the draft and executed the experiment.

Sources of Funding for Research Presented in a Scientific Article or Scientific Article Itself

This research was supported by the National Science and Technology Council, Taiwan, and JST Japan Collaborative Research Program, Grant Number: NSTC 113-2923-E-324 -001 -MY3, Grant Number JPMJKB2311, Japan.

Conflict of Interest

This experiment was approved by the Research Ethics Committee of Chung Shan University Hospital (No. CS2-21194), in Taichung, Taiwan.